References

[1] Lindquist, C. R., "Superinsulation Systems for Cryogenic Test Tank," NASA Contract NAS8-11740, June 1964–Jan. 1966, Union Carbide Corp., Huntsville, Ala.

[2] Coston, R. M., "A Study on High-Performance Insulation Thermal Design Criteria," NASA Contract NAS8-20358, Vol. 1, June 1967, Lockheed Missiles & Space Co., Sunnyvale, Calif.

[3] Hyde, E. H., "Multilayer Insulation Thermal Protection Systems Technology," TMX-64561, Rep. 2, Vol. 4, 1972, NASA.

[4] Brogan, J. J., "Investigation Regarding Development of a High-Performance Insulation System," NASA Contract NAS8-20758, 3rd Quarterly Rept., Nov. 1967–Feb. 1968, Lockheed Missiles & Space Co., Sunnyvale, Calif.

[5] Santeler, D. J., "Outgassing Characteristics of Various Materials," *Transactions of Fifth National Symposium on Vacuum Technology*, Pergamon Press, New York, 1958, pp. 1–8.

[6] Dayton, B. B., "Relations Between Size of Vacuum Chamber, Outgassing Rate and Required Pumping Speed," *Transactions of the Sixth National Symposium on Vacuum Technology*, Pergamon Press, New York, 1959, pp. 101–119.

[7] Glassford, A. P. M., "Outgassing Behavior of Multilayer Insulation Materials," *Journal of Spacecraft and Rockets*, Vol. 7, No. 12, Dec. 1970, pp. 1464–1468.

[8] Gill, S., "A Process for the Step-by-Step Integration of Differential Equations in an Automatic Digital Computing Machine," *Proceedings of the Cambridge Philosophical Society*, Vol. 47, 1951, pp. 96–108.

JULY 1973 AIAA JOURNAL VOL. 11, NO. 7

Experimental CW Chemical Laser Studies

D. J. SPENCER* AND R. L. VARWIG†
The Aerospace Corporation, El Segundo, Calif.

Experimental studies of The Aerospace Corporation's continuously operating diffusion-type HF chemical lasers are presented. Nonuniform flow profiles at the laser nozzle exit are deduced by the use of pitot and total-temperature probes. The presence of shock waves and the measured flow profiles were of particular interest in the explanation of laser performance under varied flow conditions. Low-diluent ratio flows resulted in a deterioration of laser performance partly because of thermal blockage effects. Alternate nozzles were plugged in order to provide lateral jet expansion relief, which resulted in improved laser performance. Pressure scaling was investigated up to approximately 5 atm plenum pressure and 16-torr cavity pressure. For fixed plenum conditions, an increase in cavity pressure resulted in a decrease in laser power and axial lasing length (due to oblique shocks and nozzle separation). For fixed cavity pressure, an increase in plenum pressure resulted in an increase in power and axial lasing length (due to a reduced boundary layer). The cavity pressure for peak power corresponded quite closely to the cavity pressure predicted for matched nozzle flow.

Nomenclature

A/A^* = nozzle area ratio
M = freestream Mach number
$\dot{m}$ = mass flow, g/sec
p = pressure
p_t' = pitot or impact pressure
r = throat semiheight
T = temperature
u = velocity
X = axial distance downstream of nozzle exit plane
X_c = axial distance downstream of nozzle exit plane to cavity optic axis
Y/Y_{CL} = normalized distance from wall-to-jet centerline along nozzle exit plane
β_F = molar ratio of diluent to atomic fluorine
β = molar ratio of diluent to molecular fluorine $= 2\beta_F$
δ = boundary-layer thickness
δ^* = local displacement thickness
η = chemical efficiency

Subscripts

c = cavity conditions
p = plenum total conditions
t = total or stagnation conditions
w = wall conditions
∞ = freestream

Presented as Paper 72-712 at the AIAA 5th Fluid and Plasma Dynamics Conference, Boston, Mass., June 26–28, 1972; submitted September 25, 1972; revision received January 11, 1973. This work reflects research supported by the Air Force Weapons Laboratory of the Department of Defense under U.S. Air Force Space and Missile Systems Organization (SAMSO) Contract F04701-72-C-0073.

Index categories: Lasers; Reactive Flows.

* Staff Scientist. Member AIAA.
† Staff Scientist. Member AIAA.

Introduction

CONTINUOUSLY operating diffusion-type HF chemical lasers have been in operation at The Aerospace Corporation since May 1969 (Ref. 1). In these facilities, a supersonic freejet containing fluorine atoms is produced by dissociating SF_6 with arc-heated N_2 in the jet plenum. Lateral diffusion of H_2 into the jet created excited HF, which was made to lase in an optical cavity. The current facility with which extensive laser studies have been made[2–8] is the 36-nozzle configuration shown in Fig. 1. In this arrangement, H_2 is injected into the flow from perforated tubes at the nozzle exits. At Aerospace, arc-heated He is now being used to dissociate the SF_6 (Ref. 8). F_2 has also been used directly in an arc-heated laser device where facilities for handling gaseous F_2 were available.

Fluid dynamic phenomena that affect laser performance are shown in Fig. 2. The flow profile at the nozzle exit is nonuniform because of the nozzle wall boundary layer. H_2 injection, the lateral expansion of the heated gas, or nozzle overexpansion may result in a shock wave upstream of the nozzle exit. Associated with this shock is some boundary-layer separation as well as a

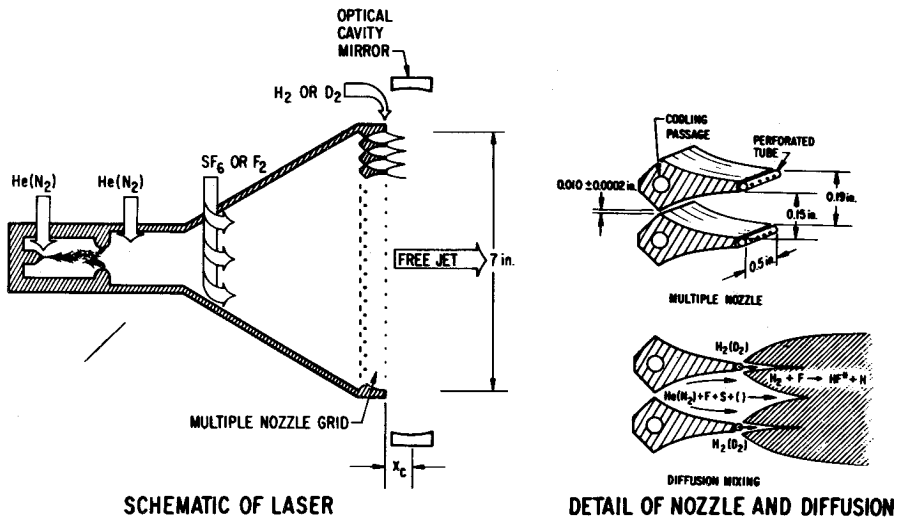

Fig. 1 Diffusion-type chemical laser with standard 36-slit nozzle.

recirculation region containing H_2, HF, F, and He. Finally, the diffusion process becomes turbulent somewhat downstream of the nozzle exit.

In an attempt to analytically predict laser performance, it is necessary to consider these fluid dynamic phenomena. Theoretical numerical[9] and analytical[10,11] solutions can be used to treat nonuniform initial profiles. laminar or turbulent mixing, and pressure gradients in the streamwise direction (due to the displacement thickness of the reaction zone). Diagnostic studies were therefore undertaken to establish the profiles of the flow at the nozzle exit and in the mixing region. In addition, in a continuing effort to improve laser performance, an examination of apparent thermal blockage of the nozzles with large F_2 concentrations was made. Finally, theoretical predictions of the effects of pressure on laser performance (power and efficiency) were examined experimentally.

In this paper, measurements of the nozzle exit flow, the thermal blockage effects, and the effects of pressure level on laser performance are reported and discussed.

Nozzle Exit Flow Study

To determine the flow properties in the flow at the nozzle exit, pitot pressure and stagnation temperature profiles were obtained.[13] Pitot-probe measurements for the case of room-temperature air at 1 atm in the arc plenum are shown in Fig. 3. The optical cavity pressure P_c was 4 torr for these tests. Pitot-pressure measurement at the center of the nozzle exit indicated the exit flow to be $M_\infty = 4.6$ or $p_\infty = 2.2$ torr. Hence, the flow was overexpanded and oblique shocks induced, as indicated by the dashed lines in Fig. 4. The peaks in the pitot-pressure profile at $X = 0.04$ in. correspond to the shock-wave location. The pitot profiles at downstream locations reflect the propagation of the oblique shocks; hence, the pitot-pressure measurements are useful in establishing cavity pressure required for pressure matching with the nozzle exit flow and for the detection of shock waves.

Pitot-pressure profiles for hot He, taken with the use of three nozzle segments, are shown in Fig. 4. The nozzle flow is almost completely viscous; i.e., the boundary layer almost fills each nozzle. In addition, the flow is overexpanded, and separation shock waves appear to originate relatively far upstream from the nozzle exit.

The stagnation temperature profile for three nozzle segments tested with heated He is shown in Fig. 5. These data were obtained with iron constantan thermocouples as described in Ref. 13. For this test, the plenum temperature measured upstream of the throat with a thermocouple is 1150°K. The temperature maximum of the nozzles is 1040°K. Thus, the recovery factor

$$[T_t\,(\text{test station}) - T_\infty]/[T_t\,(\text{plenum}) - T_\infty] = 0.9$$

is essentially the value observed by Graves and Quiel[12] for large, high-quality wind-tunnel nozzles.

The stagnation temperature profile is insensitive to the shock structure at the nozzle exit and is a direct measurement of the thermal boundary-layer thickness. As with the pitot-pressure profile, an almost completely viscous flow is observed.

Theoretical estimates of nozzle-wall boundary-layer development have been made with an existing program (Blottner) with negligible boundary-layer thickness at the throat assumed.[13] Interaction between the boundary layer and the inviscid core flow (assumed to be one dimensional) was taken into account. Results for pitot-pressure, total-temperature, velocity, and static-

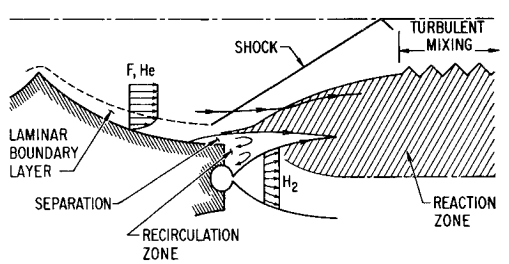

Fig. 2 Fluid dynamic phenomena in region downstream of nozzle exit.

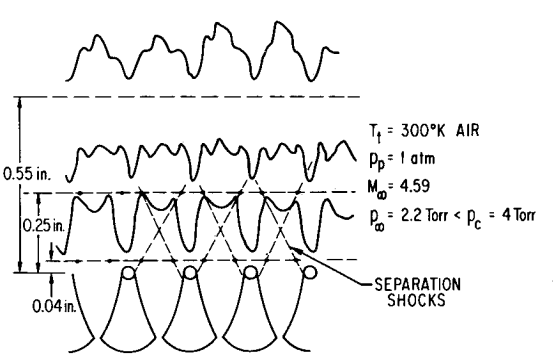

Fig. 3 Pitot-probe survey for overexpanded cold air.

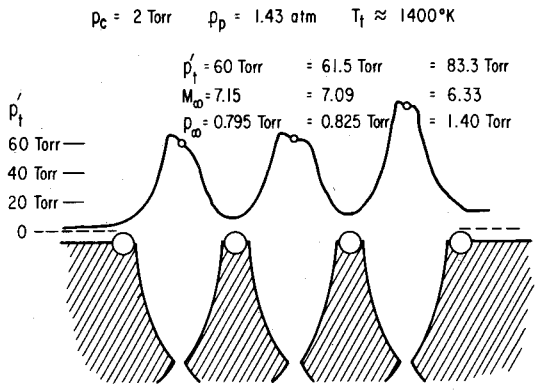

Fig. 4 Pitot-pressure profile at nozzle exit plane in He.

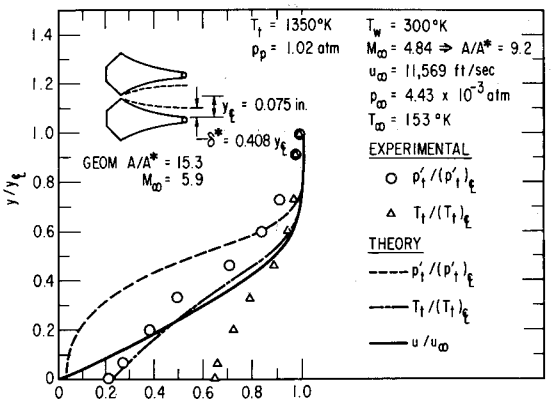

Fig. 6 Slit nozzle exit boundary-layer profiles for He.

temperature profiles are given in Fig. 6 for the case of hot He flow (there was no H_2 injection during these tests) along with corresponding experimental results (mean values) of pitot-pressure and stagnation temperature. The nozzle area ratio is 15.3 and would yield an exit Mach number of $M_\infty = 5.9$ for inviscid He flow. The theoretical estimate from the boundary-layer calculation is $M_\infty = 4.8$ because of the boundary-layer displacement thickness at the exit. The experimental value, however, is $M_\infty = 7.1$ (based on the ratio of pitot pressure to plenum pressure). The latter value indicates an effective area ratio of 25, which is larger than the geometric value of 15.3. The result indicates that viscous effects at the throat reduce the effective throat area by an amount that is larger, proportionately, than the corresponding reduction in the nozzle exit area. In the calculation of M_∞ from measured pitot pressure, it is assumed that the nozzle freestream stagnation pressure is equal to arc-plenum pressure, i.e., that some uniform flow core still exists even though the wall boundary layer is thick. If this condition is not obtained, the experimentally deduced value of M_∞ is too high.

At low pressures, the theoretical predictions are in poor agreement with the experimental observations of nozzle exit conditions (Fig. 6). Thus, experimental measurement appears to be the most reliable method for establishing exit flow conditions.

Present results with hot He indicate that optical-cavity pressures of the order of 1 torr are needed for pressure matching of the nozzle exit flow when plenum pressures are of the order of 1 atm. Most lasing tests have been conducted at cavity pressures of 2 torr (or above) because of exhaust system limitations. The flow was overexpanded for these tests, which resulted in oblique shock formation and some nozzle separation. It is expected that reduced optical-cavity pressures or increased arc-plenum pressure (>1 atm) will result in improved laser performance.

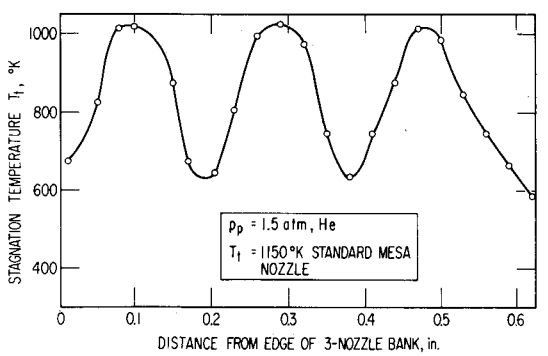

Fig. 5 Stagnation temperature profile at three nozzle segment nozzle exit plane.

Thermal Blockage Effects

It was observed in the F_2 flow laser that reduction of the ratio of diluent flow to F_2 flow ($\sim\beta$) ultimately resulted in a considerable deterioration of laser performance. This deterioration was believed to be due in part to thermal blockage effects. That is, the relatively large heat addition to the flow just downstream of the nozzle exit caused large local gas expansion, which resulted in shock waves and poor laser performance.

Static pressure measurements were made of each jet in the slit nozzle configuration in the end walls at a point 0.1 in. downstream of the hydrogen injection tubes. The nozzle and pressure tap geometry is shown in Fig. 7. These lip static pressure measurements showed an increase over the cavity static pressure for low β conditions. A decrease in laser power was always associated with this phenomenon.

The increase in the measured lip pressure is believed to be caused by the presence of oblique shocks in the nozzle. These shocks may originate either from the contoured side walls or from the flat end walls of the individual nozzles (Fig. 8). Their formation is due to the large heat addition ($\Delta T/T$ large) in the reaction zone. In a high β flow, the thermal release of the reaction causes only a small increase in the flow temperature. As the value of β is decreased, the increase in the flow temperature becomes significantly greater than the nonreacting flow temperature, causing shock generation to accommodate the change in flow density. Shock generation may also be caused by combustion in the nozzle boundary layer created by the upstream migration of hydrogen along the wall (Fig. 8). This effect may be of particular significance if the laminar boundary layer is separated due to pressure mismatch.

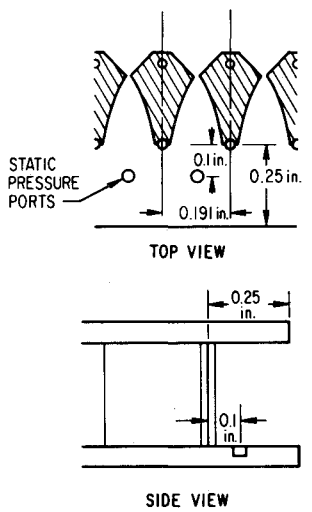

Fig. 7 Nozzle and pressure tap geometry.

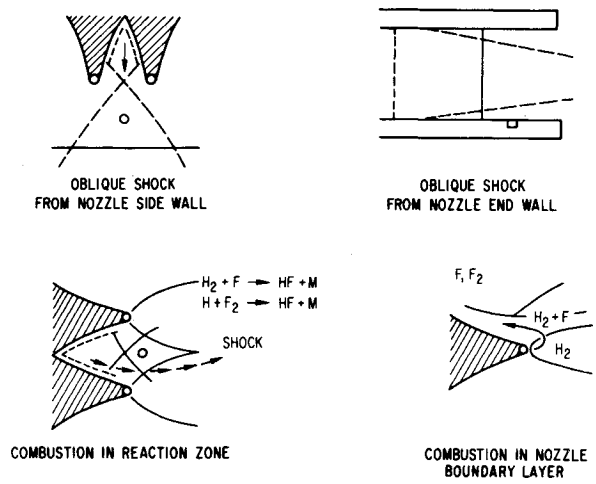

Fig. 8 Shock generation.

A proposed method for providing thermal blockage relief is the lateral expansion of the reacting gas flow into a constant-pressure or "dead" gas region. This concept is shown in Fig. 9. Recirculation of HF in the "dead" gas region should be avoided by some base bleed.

An experimental study was performed in the Aerospace laser to verify this approach. Twenty-four slits of a standard 36-slit nozzle were plugged, and the center 12 slits were left open for flow. Tests were conducted with gas flows of 2.57 g/sec He, 0.8 g/sec O_2, 1.0 g/sec H_2, and variable amounts of SF_6. The SF_6 flow rate was varied from 0.75 to 1.5 to 3.4 g/sec. Optical-cavity pressures were in the range of 4 to 5 torr; plenum pressures were 20 to 25 psia. Closed-cavity calorimeter power was measured as a function of the optical-cavity centerline position X_c for the three SF_6 flow rates. The data are plotted in Fig. 10. Peak power for $\dot{m}_{SF_6} = 0.75$ g/sec was 300 w. For $\dot{m}_{SF_6} = 1.5$ g/sec, it was 580 w; i.e., the power was proportional to the F mass flow. The X_c value for peak power was not critical over a broad range for both mass flows, i.e., from 0.7 to 1.5 in. However, calorimeter power was only 530 w for the 3.4 g/sec SF_6 flow. In addition, the X_c value that yielded peak power had moved upstream to 0.4 in. The nozzle was then replugged such that 12 alternate slits were open for flow and the intermediate slits were closed. Hence, each nozzle segment with flow was bounded by nozzle segments without flow, the latter providing a "dead" gas region at their exits. The H_2 tubes were all operating so that H_2 was available for reaction on each side of the fluorine nozzles as normally obtained.

Closed-cavity calorimeter power was again measured as a function of X_c for three different SF_6 mass flows. These data are plotted in Fig. 10. The $\dot{m}_{SF_6} = 0.75$ and $\dot{m}_{SF_6} = 1.5$ g/sec flows yielded peak powers of 376 and 700 w, respectively. These power levels are approximately 20 to 25% higher than the values in the previous test. The $\dot{m}_{SF_6} = 3.4$ g/sec peak power was 1080 w

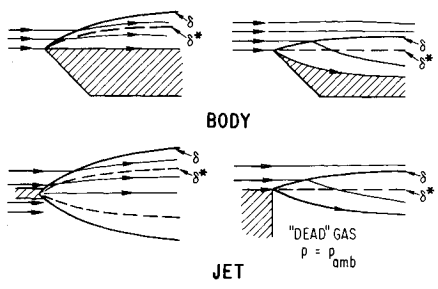

Fig. 9 Pressure relief concepts.

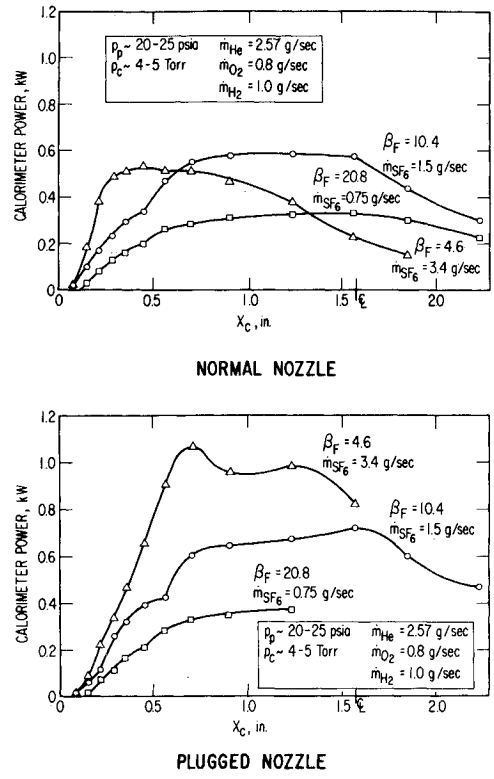

Fig. 10 Power as function of mass flow.

at $X_c = 0.7$ for the second configuration. Thus, a dramatic increase in output power was measured for the high SF_6 mass flow. [These power levels are below those reported in Ref. 8, probably due to the reduced lasing width (effectively 2.3 in.) that leads to unsaturated laser performance.] The thermal blockage relief concept is probably valid.

Thereafter, an enlarged expansion region was provided for the reacting flow in the F_2 flow laser by plugging alternate nozzle slits in the 7-in. slit nozzle configuration in order to provide flow pressure relief. The onset of pressure increase occurs at a lower value of β than with the full nozzle array, which also indicates the effectiveness of this technique.

Pressure Effects

Initially, all laser test were conducted such that the arc-plenum pressure was of the order of 1 to 2 atm and the laser cavity pressure was 3 to 5 torr. This low-cavity pressure required the use of pumps in order to exhaust the flow to atmospheric pressure. It would be desirable to raise the pressure level in the plenum and cavity in order to reduce pumping requirements. However, idealized theoretical considerations suggest that laser efficiency η varies as p_c^0 for $p_c < 0.3(\beta)^{1/2}$ (instantaneous mixing model) and inversely with p_c for $p_c \geq 0.3(\beta)^{1/2}$ (diffusion limited model). The corresponding power dependence is $Pwr \sim p_c$ and p_c^0, respectively.[9-11] Hence, it is of interest to experimentally investigate the effects of pressure level on laser performance and to see if scaling laws exist that will aid in system studies.

Limitations on arc power available for SF_6 dissociation prevented high-pressure operation with full-scale nozzles. However, in an initial effort to determine high-pressure operational characteristics, a standard 36-slit nozzle was plugged such that only the central five nozzles were left open for flow. An ATJ graphite liner was inserted into the arc heater plenum to duct the hot SF_6–He flow to the five nozzle slits and to reduce convective heat loss to the plenum walls. The graphite duct served well as a hot wall liner and reached operating temperature in a few seconds. Inclusion of the graphite duct in the system per-

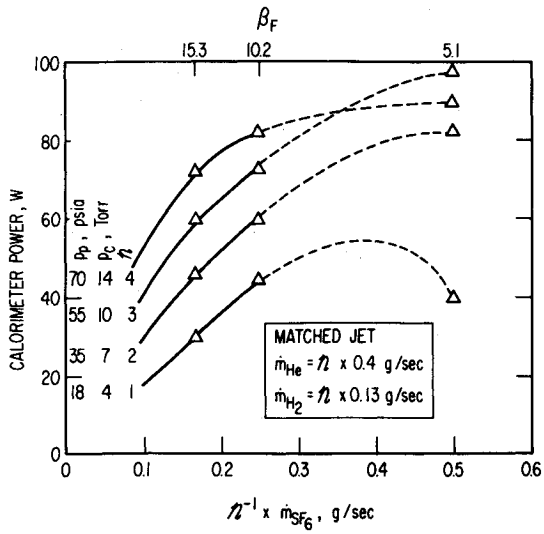

Fig. 11 Effect of pressure level on power for standard slit nozzle with five slits open.

mitted operation at a higher pressure. Material loss was minimal, except when O_2 was introduced upstream. The test series was therefore performed without O_2. A jet catcher of $2\frac{1}{2}$ in. inlet diameter was mounted 6 in. downstream of the jet in order to reduce recirculation of ground-state HF in the optical-cavity region.

Calorimeter power was first measured for the following conditions: $\dot{m}_{He} = 0.4$ g/sec; $\dot{m}_{H_2} = 0.13$ g/sec; $\dot{m}_{SF_6} = 0.17, 0.25$, and 0.5 g/sec; $p_p = 18$ psia; and $p_c = 4$ torr. Thereafter, the mass flows were all doubled. A minor adjustment was then made to the power supply in order to achieve a p_p double the previous value. This ensured a similar T_p and thus dissociation level. This procedure was repeated for mass flows both three and four times the initial mass flows. Plenum pressures ranged from 18 to 70 psia. X_c was varied for maximum power for each pressure level, but proved to be insensitive. The data are presented in Fig. 11. Since all mass flows were increased proportionally in the four test runs, all test points correspond to one of three dilution levels: $\beta_F = 5.1$, 10.2, and 15.3. These are also given in Fig. 11. The $\beta_F = 5.1$ data points show inconsistencies, which may be evidence of differences in dissociation level. The higher β_F points (corresponding to lower SF_6 flow rates) show a consistent monotonic pattern and are in those portions of the curve that correspond to complete

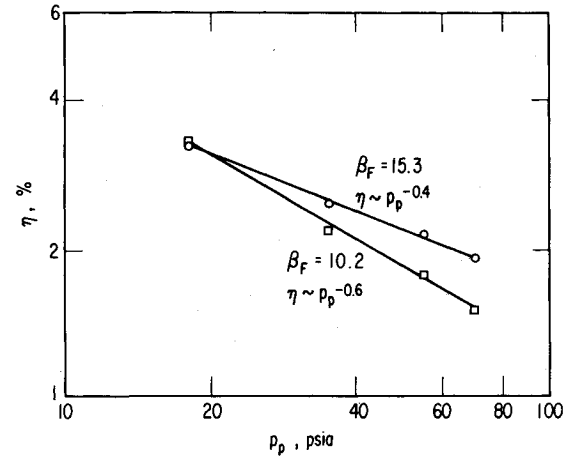

Fig. 12 Effect of pressure level on efficiency for standard slit nozzle with five slits open.

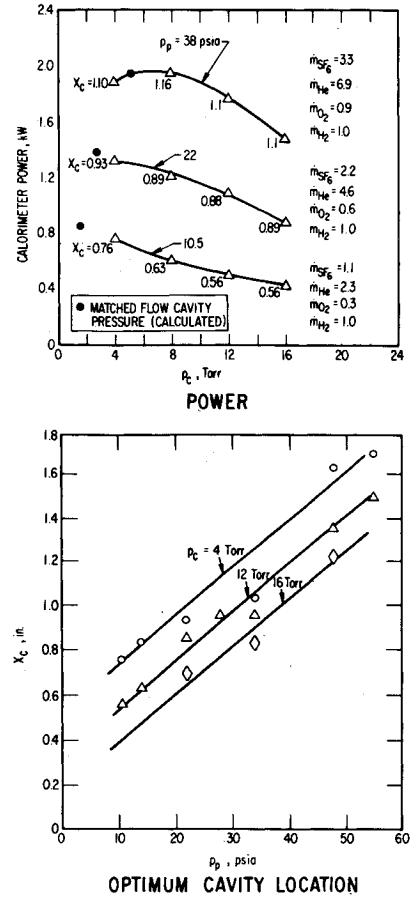

Fig. 13 Effect of pressure for standard slit nozzle with 36 slits open.

dissociation. The stepwise increase in power with each increase in pressure is apparent.

The effect of p_p on efficiency is plotted for the $\beta_F = 10.2$ and $\beta_F = 15.3$ data points in Fig. 12. The curves have the form $\eta \sim p_p^{-0.6}$ and $\eta \sim p_p^{-0.4}$, respectively. These results may be compared with the result $\eta \sim p_c^{-1}$ for a diffusion-limited laser in which initial nozzle boundary-layer effects are negligible and the result $\eta \sim p_c^{0}$ for a premixed laser, i.e., one in which the diffusion is fast in comparison with collisional deactivation. The variation of η with p, between the limits of $\eta \sim p_c^{0}$ and $\eta \sim p_c^{-1}$, can be deduced from Ref. 11. The present results are intermediate between these limits and have the expected trend that the exponent decreases with a decrease in β. The laser efficiency level is low by a factor of ~ 3 for comparable 1-atm data previously obtained. This is probably due to unsaturated operation caused by the greatly reduced optical path length of this test configuration (5 slits vs 36 slits, i.e., 1 in. vs 7 in.).

Further arc-heater efficiency improvement permitted some pressure effect studies with full-scale nozzle configurations. p_c was varied for each of several values of p_p.

The effect of pressure level on the performance of the standard slit nozzle is indicated in Fig. 13. Closed-cavity power is presented as a function of p_c for several values of p_p and several plenum mass flows. Corresponding optical-cavity centerline locations X_c are included. For $p_p = 10.5$ psia and $\dot{m}_{SF_6} = 1.1$ g/sec, the power and cavity length both increased as p_c was reduced from 16 to 4 torr. Additional increases in power and X_c would have been expected if p_c had been reduced further. However, this was not possible because of pumping limitations. An inviscid calculation of matched-flow cavity pressure for the experimental values of p_p are given in Fig. 13. The penalty due to pressure mismatch is also shown in Fig. 13. An increase in p_c above the matched value causes oblique shocks and nozzle flow separation, which reduces laser power and X_c. Similar trends are shown for $p_p = 22$ psia and $\dot{m}_{SF_6} = 2.2$ g/sec. However, the nozzle exit flow

appears to be more nearly matched at $p_c \approx 4$ torr. When $p_p = 38$ psia and $\dot{m}_{SF_6} = 3.3$ g/sec, the power reaches a maximum at $p_c = 8$ torr, which is close to the calculated matched condition. Hence, the variation of laser performance with pressure level is quite complex, and scaling laws appear to be meaningful primarily when p_c is matched, or almost matched, with nozzle exit pressure and when the nozzle boundary layer is small. The ratio of p_p to p_c for matched conditions is a complex question and depends on the plenum Reynolds number as well as nozzle geometry. Because of facility limitations, there does not appear to be sufficient range in the data of Fig. 13 to permit conclusions regarding pressure scaling laws for matched operation.

The variation of X_c with p_p for fixed values of p_c is given in Fig. 13. X_c is shown to increase with increases in p_p (due to reduced nozzle boundary layer) and to decrease with increases in p_c (due to oblique shocks and nozzle separation).

Conclusions

Nonuniform flow profiles at the diffusion laser nozzle exit have been deduced from measurements with pitot probes and total-temperature probes. The measured profiles and the presence of shock waves in the flow were of particular interest in the explanation of laser performance under varied flow conditions. There is a need for further flow diagnostics in order to determine actual flow profiles at various plenum and cavity conditions. Low-diluent ratio flows resulted in a deterioration of laser performance partly because of thermal blockage effects. Alternate nozzles were plugged in order to provide lateral jet expansion relief, which resulted in improved laser performance.

Pressure scaling was investigated up to approximately 5-atm plenum pressure and 16-torr cavity pressure. Efficiency exhibited a trend proportional to $p^{-0.6}$ and $p^{-0.4}$ depending on β, with the predicted trend of decreasing exponent with decreasing β. For fixed-plenum conditions, an increase in cavity pressure resulted in a decrease in laser power and axial lasing length (due to oblique shocks and nozzle separation). For fixed cavity pressure, an increase in plenum pressure resulted in an increase in power and axial lasing length (due to a reduced boundary layer). The cavity pressure for peak power corresponds quite closely to the cavity pressure predicted for matched nozzle flow.

References

[1] Spencer, D. J., Jacobs, T. A., Mirels, H., and Gross, R. W. F., "Continuous-Wave Chemical Laser," *International Journal of Chemical Kinetics*, Vol. 1, 1969, pp. 493–494.

[2] Spencer, D. J., Mirels, H., Jacobs, T. A., and Gross, R. W. F., "Preliminary Performance of a CW Chemical Laser," *Applied Physics Letters*, Vol. 16, 1970, pp. 235–237.

[3] Spencer, D. J., Mirels, H., and Jacobs, T. A., "Comparison of HF and DF Continuous Chemical Lasers; I. Power," *Applied Physics Letters*, Vol. 16, 1970, pp. 384–386.

[4] Kwok, M. A., Giedt, R. R., and Gross, R. W. F., "Comparison of HF and DF Continuous Chemical Lasers; II. Spectroscopy," *Applied Physics Letters*, Vol. 16, 1970, pp. 386–387.

[5] Spencer, D. J., Mirels, H., and Jacobs, T. A., "Initial Performance of a CW Chemical Laser," *Optical Electronics*, Vol. 2, 1970, pp. 155–160.

[6] Mirels, H. and Spencer, D. J., "Power and Efficiency of a Continuous HF Chemical Laser," *IEEE Journal Quantum Electronics*, Vol. QE-7, No. 11, 1971, pp. 501–507.

[7] Spencer, D. J., Durran, D. A., and Bixler, H. A., "Continuous Chemical Laser Cavity Studies," *Applied Physics Letters*, Vol. 20, No. 4, 1972, pp. 164–167.

[8] Spencer, D. J., Mirels, H., and Durran, D. A., "Performance of CW HF Chemical Laser with N_2 or He Diluent," *Journal of Applied Physics*, Vol. 43, 1972, pp. 1151–1157.

[9] King, W. S. and Mirels, H., "Numerical Study of a Diffusion-Type Chemical Laser," *AIAA Journal*, Vol. 10, No. 12, Dec. 1972, pp. 1647–1654.

[10] Hofland, R. and Mirels, H., "Flame Sheet Analysis of CW Diffusion Type Chemical Laser," *AIAA Journal*, Vol. 10, No. 4, April 1972, pp. 420–428.

[11] Mirels, H., Hofland, R., and King, W. S., "Simplified Model of CW Diffusion Type Chemical Laser," *AIAA Journal*, Vol. 11, No. 2, Feb. 1973, pp. 156–164.

[12] Graves, J. C. and Quiel, N. R., *Impact Pressure and Total Temperature Interpretation at Hypersonic Mach Number*, Memo 20, 1954, Guggenheim Aeronautical Lab., California Inst. of Technology, Pasadena, Calif.

[13] Varwig, R. L., *Chemical Laser Nozzle Flow Diagnostics*, TR-0172(2779)-1, Feb. 1972, The Aerospace Corp., El Segundo, Calif.